Journal of Electroanalytical Chemistry 673 (2012) 1–7

Contents lists available at SciVerse ScienceDirect

Journal of Electroanalytical Chemistry

journal homepage: www.elsevier.com/locate/jelechem

Formation, characterization and electrocatalytic activity of layer-by-layer self-assembled films containing polyoxomolybdate over Au surfaces

Edgar Völker, Ernesto J. Calvo, Federico J. Williams *

Departamento de Química Inorgánica, Analítica y Química-Física, INQUIMAE-CONICET, Facultad Ciencias Exactas y Naturales, Pabellón 2, Ciudad Universitaria, Buenos Aires CP1428, Argentina

ARTICLE INFO

Article history:
Received 20 December 2011
Received in revised form 17 March 2012
Accepted 23 March 2012
Available online 3 April 2012

Keywords:
Polyoxomolybdate
Layer-by-layer
Self assembly
Ion exchange
Electrocatalysis

ABSTRACT

We describe a novel strategy for the controlled fabrication of well-defined multilayer films incorporating a polyoxomolybdate anion ($PMo_{12}O_{40}^{3-}$, POM) via ion exchange on Au electrodes. Composite films were thoroughly characterized by ellipsometry, X-ray photoelectron spectroscopy (XPS), FTIR-ATR, quartz crystal microbalance (QCM) and cyclic voltammetry (CV). XPS and FTIR-ATR measurements showed that the Keggin structure of polyoxomolybdates is maintained as they are incorporated into the film. QCM experiments demonstrated that larger amounts of POM are incorporated into thicker film electrodes. EQCM and XPS measurements further showed that part of the film is delaminated when the modified electrodes were submerged in acid or basic solutions, but after this initial loss of mass the electrodes remain stable in time and with electrochemical use. POM-modified electrodes showed a pH-dependent electrochemical behavior, with peak potentials shifting by -60 mV pH^{-1}, characteristic of a $2e/2H^+$ redox process at room temperature. Furthermore, our results suggest that POM molecules in the film are not decomposed when the electrodes are immersed in solutions with pH = 4.8 a key finding as POM molecules in solution suffer from complete hydrolysis at this pH value. Finally, the performance of these POM-modified electrodes as electrocatalysts was assessed via the reduction of nitrite, chlorate and peroxodisulfate.

1. Introduction

Electrode modification is a widely spread research area that has been continuously growing in the last 20 years. Research in this field is mainly driven by the broad range of applications in light-to-energy conversion, bio-analytical processes and electrocatalysis in which they play a key role. Furthermore it is also driven by our need to understand electron transfer reactions in depth. Conducting or semiconducting electrodes can be chemically modified with a diverse set of molecules including redox active species such as inorganic complexes, conductive and nonconductive polymers and/or a combination of them [1]. In the last 15 years, the importance of polyoxometalates in the manufacture of chemically modified electrodes has been recognized. Polyoxometalates constitute a large category of polyoxoanions of mainly molybdenum, tungsten and, to a lesser degree, vanadium. Heteropolyanions and their metal-substituted derivatives have some useful properties, such as the high stability of most of their redox states, the possibility of fine tuning their redox potentials without affecting their structure, and the possibility of multiple electron transfer. These properties make heteropolyanions attractive as redox catalysts for indirect electrochemical processes [2,3], corrosion inhibitors [4], etc. Among the large family of polyoxometalates, some heteropolyanions with Keggin or Dawson structures have the ability to proceed in multiple, consecutive, and reversible multi electron reductions to mixed-valence species without decomposition. The heteropolyanions have long-term chemical stability with good ionic and electronic conductivity, which are useful and attractive in modification of electrode surfaces. However, one of the mayor drawbacks some polyoxometalates have is their limited pH-stability. For example polyoxomolybdates are known to decompose in solution: they undergo several hydrolyses reactions as the pH increases above 2 realizing MoO_4^{2-} and PO_4^{2-} anions.

Attaching redox-active polyoxometalates onto electrodes simplifies their electrochemical studies and facilitates their applications in many fields. A number of strategies have been developed to modify electrodes with a variety of heteropolyanions, such as (i) adsorption on electrode surfaces [5–7], (ii) electrodeposition at a sufficiently negative potential [8,9], (iii) doping in conductive [10], and nonconductive polymers [11,12], and (iv) other strategies [13–17]. Many authors have used chemically modified electrodes to study the properties of polyoxometalates as heterogeneous catalysts. Studies were made on the reduction of nitrite [14–18], chlorate [14,16,19], bromate [14,16,20], hydrogen peroxide [16,20,21], and oxygen [14,19].

* Corresponding author. Tel.: +54 11 45763378; fax: +54 11 45763341.
E-mail address: fwilliams@qi.fcen.uba.ar (F.J. Williams).

1572-6657/$ - see front matter © 2012 Elsevier B.V. All rights reserved.
http://dx.doi.org/10.1016/j.jelechem.2012.03.014

The Layer-by-Layer (LbL) self-assembly technique has been used to form organized multilayers with well-defined morphological characteristics in the past [22]. The method is based on the electrostatic interaction between oppositely charged species that are used to build up a variety of multilayer assemblies on a layer-by-layer basis with precise control of the thickness and layer sequences [22–25]. In particular, electrochemically active polyelectrolyte multilayers have been investigated, both with covalently bound electron donor/acceptor sites in the polymer backbone or with soluble redox ionic species doping the polycation–polyanion structure [26]. Among the redox active polyelectrolyte multilayers two different systems have been studied: (i) the acceptor/donor redox site covalently attached to the polyelectrolyte backbone, i.e. ferrocene, osmium pyridine complexes [27,28], and (ii) the as-formed polyelectrolyte multilayer exchanges redox active ions (i.e. hexacyanoferrate [28], osmium bipyridinium [29]) from the electrolyte solution by breaking polycation–polyanion bonds and making polyion-redox ion bonds in the structure [28]. Multilayered molecular assemblies composed of polyoxometalates and large water-soluble polycation species have been built up in the past [20,30–32] using these strategies.

In this article, we describe a novel strategy for the controlled fabrication of multilayer films containing a polyoxomolybdate anion ($PMo_{12}O_{40}^{3-}$, (POM)) on Au electrodes. Firstly, the Au substrate is covered with a well-defined layer-by-layer polyelectrolyte film and once the polyelectrolyte multilayer has been built, the POM is incorporated in the film by ion exchange [33,34]. The resulting functionalized electrodes were thoroughly characterized by ellipsometry, X-ray photoelectron spectroscopy (XPS), FTIR-ATR, quartz crystal microbalance (QCM) and cyclic voltammetry (CV). We found that POM molecules are present in the multilayer film retaining their molecular structure and that although there is an initial loss of mass when it is first submerged in acid or basic solutions, then the POM-functionalized electrodes remain stable in time and with usage. POM molecules electrochemically wired to the Au surface seem to be stable with pH, as POM molecules in the film are not hydrolyzed when electrodes are exposed to solutions with pH = 4.8. Finally, our POM-functionalized electrodes present a very good response towards the electrocatalytic reduction of nitrite, chlorate and peroxodisulfate.

2. Experimental

2.1. Reagents and materials

All solutions were prepared with 18 MΩ Milli-Q (Millipore) water. Sodium 3-mercapto-1-propanesulfonate (MPS) (technical grade, 90%, Aldrich), Poly(allylamine hydrochloride) (PAH) (average M_w 56,000, Aldrich), Poly(acrylic acid) (PAA) (average M_w 100,000, Aldrich) and phosphomolybdic acid (POM) ($H_3PMo_{12}O_{40} \cdot xH_2O$, Sigma–Aldrich) were used without further purification. Layer-by-layer films were prepared from 20 mM aqueous solutions of PAH and PAA and 5 mM aqueous solutions of $H_3PMo_{12}O_{40}$. The polymer solutions pHs were adjusted to 4.3 by addition of 0.1 M NaOH or 0.1 M HCl aqueous solutions. POM solution had a pH value close to 1.8 as prepared and was not further modified. Chemicals employed in electrolyte solutions, H_2SO_4, glycine, HCl, $NaNO_2$, $KClO_3$ and $K_2S_2O_8$, were of analytical grade and used as received.

2.2. Surface modification

Gold substrates were prepared by Au evaporation over Si wafers as discussed elsewhere [35]. As a first step they were immersed for one hour in a 50 mM MPS in 10 mM H_2SO_4 solution. This procedure creates a self-assembled monolayer terminated in sulfonate groups thus leaving the Au surface negatively charged, so the layer-by-layer deposition started with the PAH polycation. The subsequent layers were deposited on the modified surface by alternate immersion in a solution of the respective polyanion (PAA) or polycation (PAH) at pH = 4.3 in both cases for 15 min and rinsing with Milli-Q water until the desired number of layers was achieved. Finally, the substrate was further modified with a final layer of PAH, then was immersed in POM solution for at least 1 h and then rinsed with Milli-Q water. As expected, if the layer-by-layer process ended with a PAA layer, then no incorporation of POM was achieved by this method. Electrodes are named Au/MPS/(PAH_{n+1}/PAA_n)/POM where n is the number of deposited PAH-PAA bilayers.

2.3. Ellipsometry

Ellipsometric experiments were performed with a variable angle rotating analyzer automatic ellipsometer (SE 400 model, Sentech GmbH, Germany) equipped with a 632.8 nm laser as polarized light source. Measurements were carried out ex situ at a given fixed angle of 70.00°. After each adsorption step, the sample was rinsed with Milli-Q water and dried with N_2 and the ellipsometric parameters (ψ and Δ) were collected manually. All adsorption, rinsing and drying steps were carried out avoiding any variations of the electrode position in order to keep the system alignment. The ellipsometric angles were fitted with a three-layer model (air/film/substrate) [36].

2.4. X-ray photoelectron spectroscopy

XPS measurements were performed under UHV conditions (base pressure < 5×10^{-10} mbar) in a SPECS UHV spectrometer system equipped with a 150 mm mean radius hemispherical electron energy analyzer and a nine channeltron detector. XPS spectra were acquired at a constant pass energy of 20 eV using an un-monochromated Mg Kα (1253.6 eV) source operated at 12.5 kV and 20 mA and a detection angle of 30° with respect to the sample normal on grounded conducting substrates. Quoted binding energies are referred to the Au $4f_{7/2}$ emission at 84 eV. No charge compensation was necessary and no differential charging features were observed (e.g. low binding energy tails) given that we have measured sufficiently thin films on grounded conducting substrates. Atomic ratios were calculated from the integrated intensities of core levels after instrumental and photoionization cross section corrections [37].

2.5. FTIR-ATR

FTIR-ATR experiments of the Au/MPS/(PAH_{n+1}/PAA_n)/POM electrodes were carried out on a Thermo Nicolet 8700 (Nicolet, Madison, WI) spectrometer equipped with a C (diamond) SmartOrbit Thermo ATR accessory and DTGS detector (Nicolet).

2.6. Electrochemical quartz crystal microbalance (EQCM)

A quartz crystal resonator of 10 MHz was used as a QCM, which has been described elsewhere [38]. The crystals were mounted in the cell by means of viton O-ring seals, with only one face in contact with the electrolyte; this electrode was a common ground to both the AC and DC circuits. Quartz crystal shear resonator dissipation studies of the multilayer films studied in this work have shown that they behave as acoustically thin films and therefore the resonant frequency shifts can be related to mass changes by the Sauerbrey equation [39].

2.7. Electrochemical experiments

Cyclic voltammetry measurements were carried out at room temperature with an Autolab PGSTAT 30 potentiostat (Autolab, Echochemie, Netherlands). Experiments were performed in a purpose built three-electrode Teflon cell, with an electrode area of approximately 0.25 cm^2 delimited by an inert O-ring. An Ag/AgCl electrode (3 M KCl (0.210 V vs. NHE)) was employed as the reference electrode and all electrode potentials herein are quoted with respect to it. A platinum gauze of large area was used as auxiliary electrode. The Au electrodes were electrochemically cleaned by cycling the voltage between 0 and 1.6 V at 10 V s^{-1} several times in a 2 M H_2SO_4 solution, followed by a scan at 0.1 V s^{-1} to ensure surface cleanness. The electrochemically active area was estimated from the gold oxide reduction peak [40]. The pH of the supporting electrolyte solution was controlled with a 0.1 M Glycine–HCl buffer in the range 1.1–4.8.

3. Results and discussion

3.1. Incorporation of POM into LbL films

Polyoxomolybdate anions have been incorporated into PAH-PAA self-assembled multilayer films by ion exchange. The resulting Au/MPS/(PAH_{n+1}/PAA_n)/POM electrodes were characterized by ellipsometry, XPS, FTIR-ATR, quartz crystal microbalance and cyclic voltammetry. Fig. 1 shows the ellipsometric film thickness as a function of the number of deposited layers. Odd (even) numbers correspond to self-assembled layers terminated in a PAH (PAA) layer. The last data point corresponds to the addition of POM by ion exchange. Clearly, increasing the number of assembled layers results in a thickness increase which suggest a layer-by-layer growth as previously reported by Shiratori and Rubner [41].

The last data point in Fig. 1 clearly shows that the PAH/PAA self-assembled film thickness increases after the addition of POM molecules by ion exchange. This is mainly due to the incorporation of bulky POM anion and water molecules into the film [42]. Incorporation of POM into the film was demonstrated by XPS measurements as discussed below.

The surface chemical composition of the Au/MPS/(PAH_{n+1}/PAA_n)/POM with $n = 2$, 3 and 4 was determined by XPS. Broad spectra show the presence of the expected elements: Mo, P, O, C, N, S and Au. Fig. 2 shows the Au 4f, Mo 3d, N 1s and Mo 3p XP spectra corresponding to multilayer films of increasing thickness, i.e. $n = 2$, $n = 3$ and $n = 4$. Clearly, as the number of layers n increases the Au 4f XP signal decreases. This is due to the increased attenuation of the photoelectrons emitted by the Au atoms by the growing polyelectrolyte overlayer. It follows that film thickness increases with the number of deposited layers in agreement with the ellipsometric results discussed above. The Mo 3d and 3p XP signals increase as the number of deposited layers n increases, therefore more phosphomolybdic acid is incorporated into the film with increasing n. Furthermore the Mo 3d peak position (Mo $3d_{5/2}$ at 232.3 eV and Mo $3d_{3/2}$ at 235.4 eV) indicates that Mo atoms are in a +6 oxidation state as expected. Also, XPS shows that the atomic ratio Mo:P is approximately equal to 12:1 suggesting that the Keggin structure is maintained as the polyoxomolybdate is incorporated in the film. Finally, the N 1s signal (400 eV) which partially overlaps with the Mo $3p_{3/2}$ (398.1 eV) signal indicates the presence of the amine groups in the PAH polyelectrolyte and its intensity increases with increasing number of layers as expected. The atomic ratio Mo:N is approximately equal to 1:2 in all cases, i.e. there is approximately 1 POM molecule every 24 N atoms in the films, indicating that as we increase the number of amine sites in the multilayered film (and hence film thickness) the amount of POM molecules incorporated increases. In short, XPS measurements confirm the increased thickness of multilayer films with number of deposited layers and demonstrate the incorporation of increasing amounts of polyoxomolybdate anions with film thickness. Although POM ions are relatively big we should bear in mind that the films incorporate also large amounts of water and are very porous hence creating possible diffusion pathways for the incorporation of the anion. Further evidence regarding incorporation of the polyoxomolybdate heteropolyanion into the film is given by the FTIR measurements discussed below.

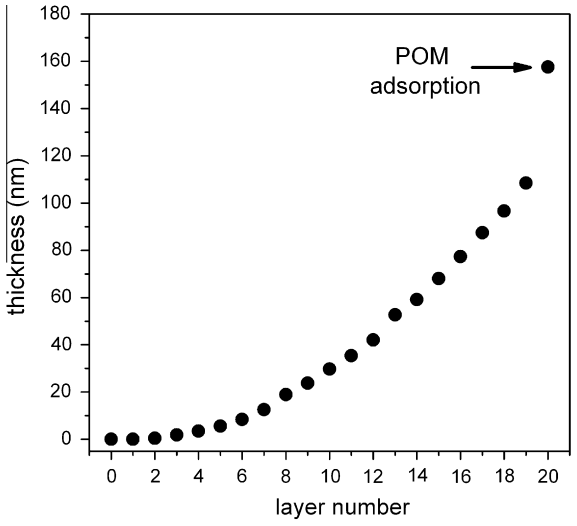

Fig. 1. Ellipsometric thickness for films prepared with PAH and PAA. The last data point corresponds to the addition of POM in the film.

Fig. 3 shows the FTIR-ATR spectrum of (a) Au/MPS/PAH_{11}/PAA_{10} multilayer self-assembled film as well as (b) the same electrode after POM incorporation by ion exchange. The amine peak (~1640 cm^{-1}) and the symmetric and asymmetric carboxylate stretching peaks (1405 and 1565 cm^{-1}) seen in Fig. 3a are clear evidence of the PAH/PAA film formation. The positions of these signals change slightly with the incorporation of POM into the film. The peaks associated to the Keggin-type polyoxomolybdate can clearly be seen in Fig. 3b: the P—O vibration belonging to the central PO_4 unit appears at about 1053 cm^{-1}. The Mo═O and Mo—O—Mo (corner sharing) vibration bands are overlapped in the multilayer film (930 and 900 cm^{-1} respectively), while the Mo—O—Mo (edge sharing) vibration band can be seen at 690 cm^{-1}. The positions of these bands are slightly shifted with respect to the compound in a KBr pellet [43,44], probably due to the interaction of the polyoxomolybdate molecules with the surrounding polyelectrolyte molecules. Clearly, IR measurements indicate that the polyoxomolybdate anions are successfully incorporated in the PAH/PAA thin multilayer film retaining their Keggin-type molecular structure.

Although XPS and FTIR-ATR measurements demonstrate the absorption of POM into the PAH/PAA multilayer films, it is not possible to easily estimate the amount of POM incorporated into the multilayer film. Therefore we carried out Quartz Crystal Microbalance (QCM) measurements in order to quantify the absorption of POM into the films. Fig. 4 shows the change in mass when two PAH_{n+1}/PAA_n samples with different number of layers ($n = 5$ and $n = 10$) are placed in contact with a solution containing POM molecules as measured by QCM. Initially the mass increases due to the incorporation of polyoxomolybdate and possibly water molecules into the films. The baseline measured after the removal of the POM solution was obtained after washing the electrode several times with Milli-Q water. The decrease in mass is probably associated with the loss of POM weakly adsorbed on the topmost layers

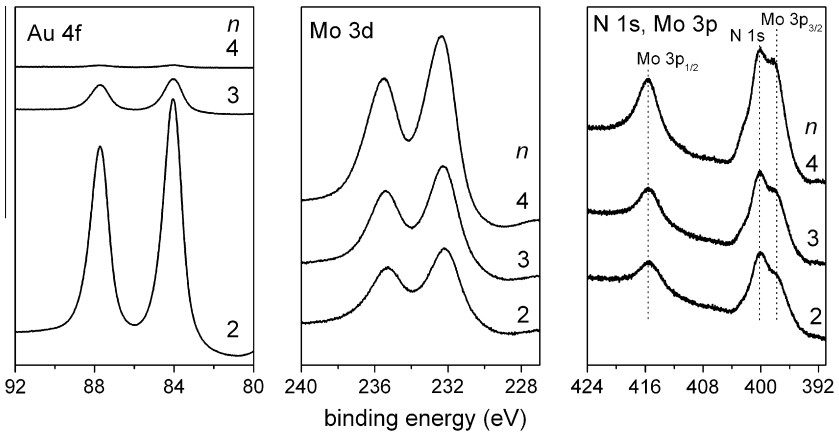

Fig. 2. Au 4f, Mo 3d, N 1s and Mo 3p XPS signals of Au/MPS/PAH_{n+1}/PAA_n/POM as a function of increasing bilayer number, $n = 2$, $n = 3$ and $n = 4$.

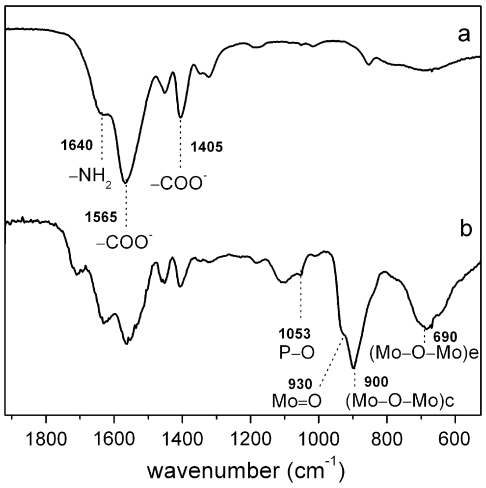

Fig. 3. FTIR-ATR spectra of (a) Au/MPS/PAH_{11}/PAA_{10} and (b) Au/MPS/PAH_{11}/PAA_{10}/POM self-assembled films.

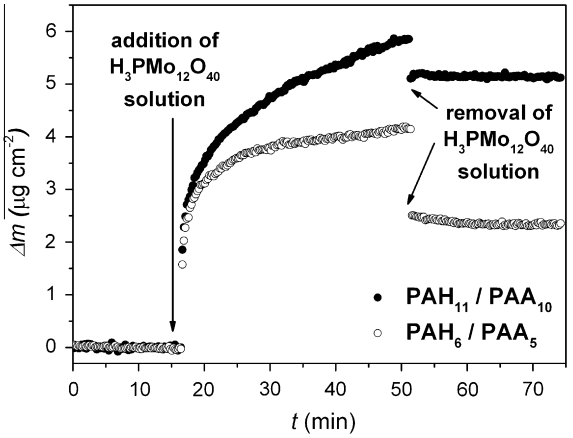

Fig. 4. QCM change in mass after the adsorption of POM on Au/MPS/PAH_6/PAA_5 (white dots) and Au/MPS/PAH_{11}/PAA_{10} (black dots).

of the film. Therefore, the adsorbed mass is estimated by subtracting the final and initial baselines.

Fig. 4 clearly shows that thicker films have a larger change in mass. FTIR and XPS measurements demonstrated the incorporation of POM molecules into the polyelectrolyte thin film. However we should not assign the observed increases in mass only to POM incorporation into the film as we cannot rule out that also water molecules absorb into the film. Therefore we carried out blank experiments to estimate the mass of water-absorption into the self-assembled PAH/PAA films. We found in all cases that approximately half the mass incorporated into the films corresponds to water molecules (note that we also measure an appreciable increase in film thickness due to water induced film swelling). Therefore a rough estimation of the mass of POM molecules absorbed into the film is approximately 1 $\mu g\,cm^{-2}$ for PAH_6/PAA_5 and 2.5 $\mu g\,cm^{-2}$ for PAH_{11}/PAA_{10}. These results can be translated into moles of POM adsorbed: 0.6×10^{-9} mol cm^{-2} for the PAH_6/PAA_5 film and 1.4×10^{-9} mol cm^{-2} for the PAH_{11}/PAA_{10} film. The adsorption of POM is clearly greater for the thicker film, a result that is in line with the XPS measurements discussed above and that is consistent with the fact that thicker films have more available absorption sites in the polyelectrolyte multilayer. Here we should note that further increases of film thickness (condition not explored in the present studies) might not lead POM incorporation increases as POM molecules need to diffuse from the surface of the self-assembled films.

3.2. Stability of LbL films containing POM

Fig. 5 shows the EQCM mass of a PAH_6/PAA_5 electrode after incorporation of POM and after immersing it in a 0.1 M H_2SO_4 solution. As discussed above (see Fig. 4) the incorporation of POM and water molecules results in a mass gain of 28% from the initial 6.8–8.7 $\mu g/cm^2$. The produced $PAH_6/PAA_5/H_2PMo_{12}O_{40}$ electrode was immersed in a 0.1 M H_2SO_4 solution resulting in a sharp mass decay to a relatively stable value of 6.5 $\mu g/cm^2$, i.e. a value even smaller than the initial mass before POM incorporation. This result suggests that POM and water as well as polyelectrolyte molecules escape the polyelectrolyte multilayer film into solution.

The inset of Fig. 5 shows two cyclic voltammetries (CV) performed on the $PAH_6/PAA_5/H_2PMo_{12}O_{40}$ electrode at different immersion times in 0.1 M H_2SO_4 solution. The observed peaks correspond to electron transfer reactions involving POM molecules as will be described in detail below (see Figs. 7 and 8), demonstrating that despite the mass loss, some POM molecules are retained in the film. Peak areas indicate that the coverage of POM molecules electrochemically wired to the Au electrode that are retained in the film is 4.1×10^{-11} mol cm^{-2}. Furthermore, notice that the second CV performed 40 min after being immersed in 0.1 M H_2SO_4 solution has the same peak currents as the first one, and notice also that after the initial mass decay the total mass remains constant with immersion time and electrochemical use. This means that once the POM-modified multilayer film has suffered loss of

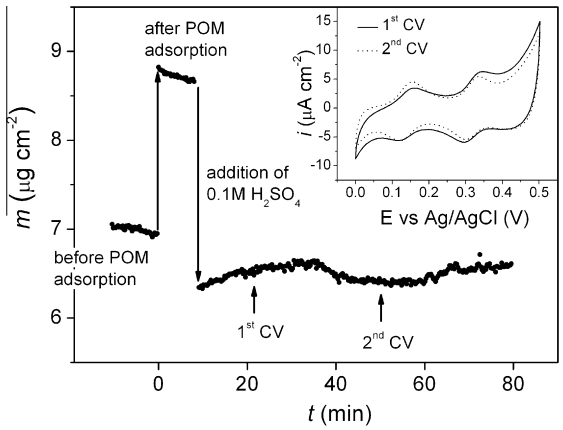

Fig. 5. EQCM mass of a Au/MPS/PAH_6/PAA_5 electrode, after absorption of POM and after immersion in a 0.1 M H_2SO_4 solution. Inset: cyclic voltammetries in 0.1 M H_2SO_4 solution, scan rate 0.1 V s^{-1}. The moment when each cyclic voltammetry was made is shown on the main graph.

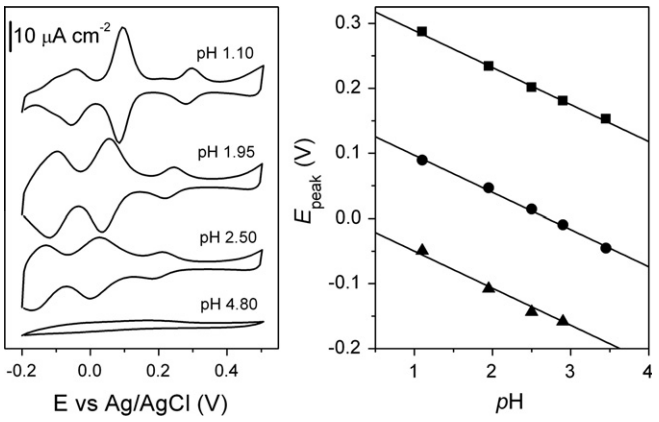

Fig. 7. Left: Cyclic voltammograms of Au/MPS/PAH_{10}/PAA_9/POM as a function of supporting electrolyte pH (0.1 M Glycine–HCl buffer, pH from 1.1 to 4.8). Right: Peak shifts as a function of supporting electrolyte pH.

material a stable film with electrochemically active POM redox sites is generated over the Au electrode with no further evidence of loss of material. Further evidence indicating the presence of POM molecules in the polyelectrolyte film after the initial loss of material is given by XPS measurements. Fig. 6 shows the Au 4f, Mo 3d, Mo 3p and N 1s XP signals before and after immersion of a PAH_5/PAA_4/POM Au substrate in a 0.1 M H_2SO_4 solution.

The Au 4f XP signal increases 85% after immersion of the polyelectrolyte multilayer in the acid solution. This indicates that the Au 4f photoelectrons are less attenuated as a result of the immersion indicating a decrease in film thickness due to partial loss of material to solution as shown by the EQCM measurements discussed in Fig. 5. Furthermore the Mo 3d and Mo 3p XP signals decrease by approximately 40% indicating that some of the polyoxomolybdate is lost from the polyelectrolyte multilayer film after the immersion. Also the N 1s XP signal arising from the PAH polyelectrolyte decreases 34% after immersion in the acid solution indicating partial delamination of the polymer film. Partial dissolution of the polyelectrolyte self-assembled film with loss of POM as well as some polyelectrolyte molecules was observed for different number of deposited bilayers (n = 3–6). However, it is important to note that in all cases after the initial sharp decrease in mass, the system does not suffer from further loss in mass and the amount of POM molecules wired to the Au electrode remains constant. Here we should note that POM-modified films are not only delaminated in acid solutions but that the same phenomenon takes place in basic

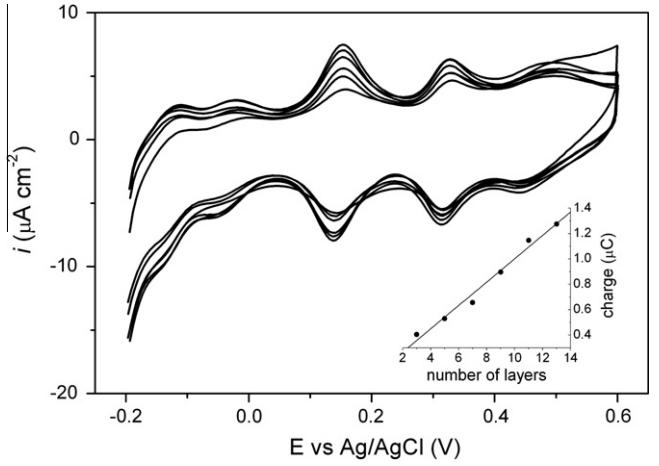

Fig. 8. Cyclic voltammograms of Au/MPS/PAH_{n+1}/PAA_n/POM (n = 1, 2, 3, 4, 5 and 6) in 0.1 M H_2SO_4 at 100 mV s^{-1}. Inset: area of third anodic peak ($E \approx 0.14$ V) as a function of the number of layers.

media. Furthermore, POM-free PAH/PAA films do not suffer from delamination either in acid or basic solutions. Therefore, we propose that incorporation of the relatively large POM anions into the LbL films increases the distance between the bilayers and thus, weakens their interaction facilitating delamination. The layers closer to the

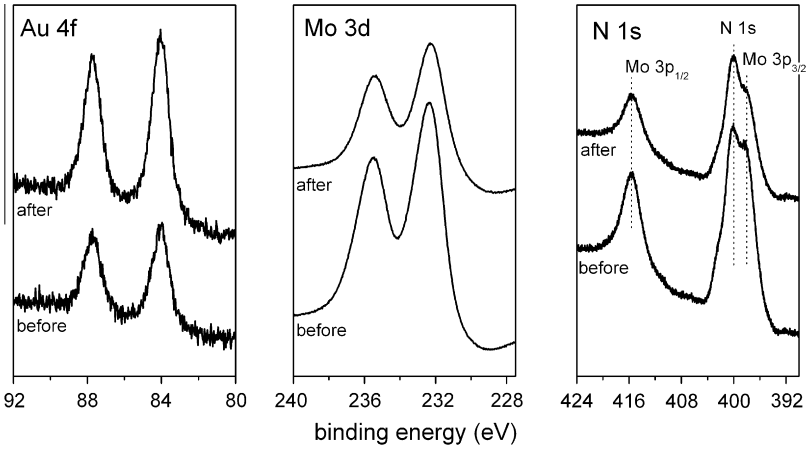

Fig. 6. Au 4f, Mo 3d, Mo 3p and N 1s XP signals before and after immersion of a PAH_5/PAA_4/POM Au substrate in a 0.1 M H_2SO_4 solution.

substrate remain attached as probably POM ions do not penetrate the film homogeneously hence not weakening to the same extent the interaction between these layers.

3.3. Electrochemical behavior of LbL films containing POM

Below we discuss the electrochemical behavior of the PAH_{n+1}/PAA_n/POM modified Au electrodes as a function of solution pH.

Fig. 7 (left) shows cyclic voltammograms (CV) of Au electrodes functionalized with PAH_{10}/PAA_9/POM as a function of supporting electrolyte pH in the range 1.1–4.8. We observe three peaks at pH 1.1 (peak I ~ 0.29 V, peak II ~ 0.09 V and peak III ~ −0.05 V vs. Ag/AgCl) whose intensity diminishes and whose positions shift to negative potentials as the pH of the electrolyte solution is increased. The same pH-dependent electrochemical behavior is commonly observed for POMs dissolved in solution or immobilized in electrodes as in the present case [17]. The dependence of peak position shift with solution pH can be explained by the fact that POM reduction is accompanied by proton transfer (from solution to the film) to maintain charge neutrality. It is thus consistent with the proposed mechanism for the oxidation–reduction peaks of $PMo_{12}O_{40}^{3-}$, which depends on pH as a result of protonation [3]:

$$PMo_{12}^{VI}O_{40}^{3-} + 2e^- + 2H^+ \rightleftarrows H_2PMo_{10}^{VI}Mo_2^{V}O_{40}^{3-}$$

$$H_2PMo_{10}^{VI}Mo_2^{V}O_{40}^{3-} + 2e^- + 2H^+ \rightleftarrows H_4PMo_8^{VI}Mo_4^{V}O_{40}^{3-}$$

$$H_4PMo_8^{VI}Mo_4^{V}O_{40}^{3-} + 2e^- + 2H^+ \leftrightarrows H_6PMo_6^{VI}Mo_6^{V}O_{40}^{3-}$$

Notice that two oxidation states Mo(VI) and Mo(V) are present with different ratios in the Keggin structure corresponding to different redox sites in the polyoxomolybdate as discussed in previous reports [45]. The pH dependence of these redox peaks follows the electrochemical reduction of Mo(VI) in the three subsequent two-electron and two-proton reversible steps shown above. Fig. 7 (right), shows the peak potential for the three successive redox waves as a function of pH for the PAH_{10}/PAA_9/POM electrode. Clearly, the three peaks shift to negative potentials as the solution pH is increased exhibiting a good linearity with a slope of about -60 mV pH^{-1}. This value is very close to the theoretical expected value of -59 mV pH^{-1} for the $2e^-/2H^+$ redox process at room temperature, which can be elucidated from the Nernst equation [46].

As shown in Fig. 7 above, as the pH increases the CV peak intensities decrease to vanish entirely at pH = 4.8. This phenomenon could be explained by two factors: (i) when solution pH increases, there is less availability of protons in solution which are necessary for the POM redox reactions [16] and (ii) when solution pH increases partial hydrolysis of POM molecules could start taking place, which should also result in smaller currents. Here we should note that reversing the solution pH from 4.8 to its original value (pH = 1.1) results in a cyclic voltammogram with the same intensity as observed originally. Therefore we can rule out hydrolysis of POM molecules in the film in the pH range 1.1–4.8 as otherwise the pH-dependent electrochemical behavior would have not been reversible. This observation can be rationalized taking into account that the pH in the local environment of the POM molecules in the film could be quite different to the solution pH. Negatively charged POM molecules are expected to be surrounded by protonated amine groups from the PAH polyelectrolyte that could be an important source of protons. This is an important suggestion as it implies that inserting POM molecules into the film broadens the pH range in which they could be used.

The surface coverage of POM on these electrodes was estimated by measuring cyclic voltammetries as a function of the scan rate (pH of supporting electrolyte = 1.1) [47]. From these measurements we estimated a coverage of POM in the PAH_{10}/PAA_9/POM functionalized Au electrode of 8.4×10^{-11} mol cm^{-2} which is remarkably smaller than the initial (before any mass loss) POM coverage estimated by QCM 1.2×10^{-9} mol cm^{-2} (see above). This implies that only ~7% of the POM initially present in the multilayer film is retained after the film is delaminated. As discussed above, the retained amount of POM molecules in the film remains constant with electrochemical use.

Fig. 8 shows cyclic voltammograms of Au/MPS/(PAH_{n+1}/PAA_n)/POM with n = 1, 2, 3, 4, 5 and 6 in 0.1 M H_2SO_4 at 100 mV s^{-1}. The inset shows the peak area of the third anodic peak (E ≈ 0.14 V) vs. the number of layers. The increase in peak area vs. the number of layers is linear, which shows that as the number of layers is increased, more electrochemically active POM is retained in the film after the initial delamination takes place. From the slope of this graph, we can estimate a growth of 5×10^{-12} mol of electrochemically active POM cm^{-2} per layer. As was shown previously with XPS and QCM experiments more POM is adsorbed on fresh films as thickness increases and therefore more electrochemically wired POM molecules are retained in the film after delamination takes place.

3.4. Electrocatalytic activity of LbL films containing POM

It is well known that reduced POM molecules are capable of delivering electrons to other species, thus serving as powerful electron reservoirs for multielectron reductions. Furthermore, direct electroreduction of nitrite, chlorate and peroxodisulfate requires a large overpotential at most bare electrode surfaces, while on the other hand, POM-modified electrodes can catalyze the electroreduction of NO_2^- [14–18,45], ClO_3^- [14,16,19], and $S_2O_8^{2-}$ [17], in aqueous solution. With these in mind, the catalytic reduction of these three molecules has been examined to evaluate the feasibility of using our POM modified electrodes in electroanalysis and electrocatalysis. Firstly we should note that POM-free PAH_{n+1}/PAA_n/Au electrodes show no electrochemical response in the presence of nitrate, chlorate or peroxodisulfate in the range 0.4 to −0.2 V vs. Ag/AgCl. However, incorporation of POM molecules into the polyelectrolyte film results in the electroreduction of nitrate, chlorate and peroxodisulfate. Fig. 9 shows the electrocatalytic reduction of (a) $NaNO_2$, (b) $KClO_3$ and (c) $K_2S_2O_8$ on $PAH_4/PAA_3/H_2PMo_{12}O_{40}$ Au electrodes in aqueous solution as a function of the increasing concentration of the reactant. With increasing concentration of NO_2^- (Fig. 9a), ClO_3^- (Fig. 9b) and $S_2O_8^{-2}$ (Fig. 9c), all three reduction peak currents increase gradually, whereas the corresponding oxidation peak currents decrease, suggesting that the three molecules are reduced by two-, four-, and six-electron reduced species of POM anions (here we should notice that the first and second reduction wave seem to be inert towards reducing ClO_3^-). Furthermore, the six-electron reduced species have a much larger catalytic activity towards reduction of the molecules than the two- and four- electron reduced species. In this reduction process, the four-electron reduced species is regenerated. The insets of Fig. 9 show the catalytic currents at the third reductive peak (−0.14 V vs. Ag/AgCl) as a function of reactant concentration. The responses of the electrodes are linear in the ranges (a) 0.50–70.00 mM, (b) 0.90–100.00 mM and (c) 0.05–0.80 mM; and the sensitivities are respectively, 0.51, 0.15 and 43.20 μA cm^{-2} mM^{-1}. These values are comparable to those found in the literature: 0.5 μA cm^{-2} mM^{-1} for NO_2^- [17], 0.74 μA cm^{-2} mM^{-1} for ClO_3^- [14] and 18.6 μA cm^{-2} mM^{-1} for $S_2O_8^{2-}$ [17]. The data shows that the POM-modified electrodes present a reasonable response towards the detection of nitrate, chlorate and peroxodisulfate. The electrodes are quite stable, yielding reproducible signals over different reactant experiments. The electrode response was stable for at least 3 weeks, and when not in use, the modified electrode was stored in air. The good stability and high sensibility

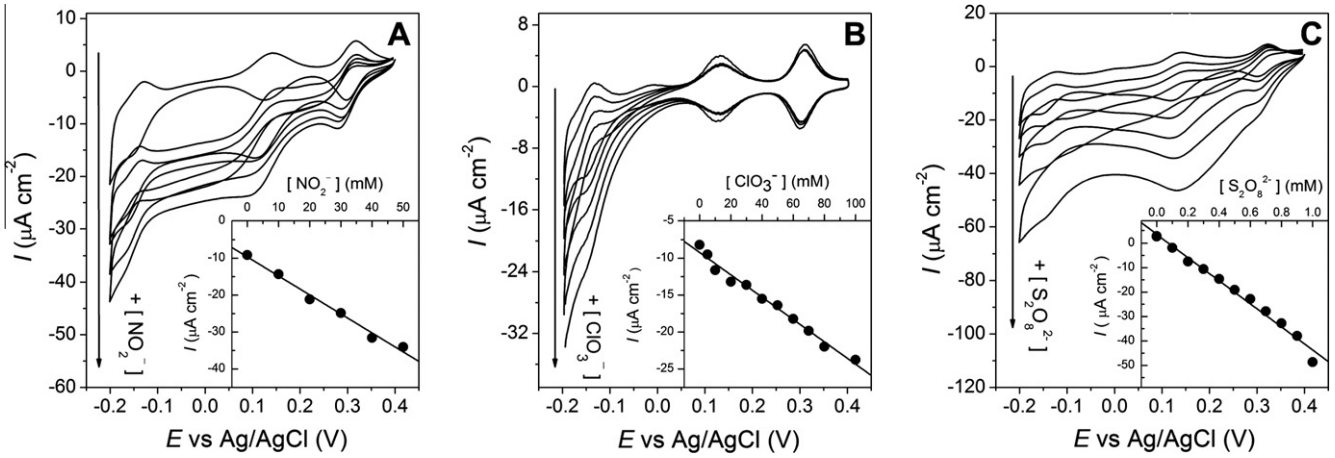

Fig. 9. Cyclic voltammetries of PAH_4/PAA_3/POM Au electrodes in the absence and presence of (a) NO_2^-, (b) ClO_3^-, (c) $S_2O_8^{2-}$. Reactant concentrations (a): 10 mM, 20 mM, 30 mM, 40 mM and 50 mM; (b): 10 mM, 30 mM, 50 mM, 70 mM, 100 mM; (c): 0.2 mM, 0.4 mM, 0.6 mM, 0.8 mM, 1 mM. Scan rate 0.025 V s^{-1}. Inset: catalytic currents at the third reductive peak (−0.14 V vs. Ag/AgCl) as a function of reactant concentration.

of these electrodes make them promising candidates for amperometric detectors.

4. Conclusions

We have developed a new, convenient and efficient method for the functionalization of layer-by-layer self-assembled polyelectrolyte films deposited over Au electrodes with polyoxomolybdate anions via ion exchange from solution. POM functionalized electrodes were thoroughly characterized with XPS, FTIR-ATR, ellipsometry and EQCM which clearly show that POM molecules can be successfully incorporated into polyelectrolyte films via ion exchange. These fresh films suffer from a sharp delamination that involves the loss of polyelectrolyte as well as POM molecules from the films into acid or basic solutions. Remarkably, after this initial sharp decrease in mass they remain stable in time and with electrochemical use. Electrochemical measurements as a function of pH suggest that POM molecules do not decompose even when the external pH is 4.8. This is an important finding as it indicates that incorporation of POM molecules into layer-by-layer self-assembled monolayer films could prevent partial hydrolysis of POM from taking place in the pH range studied. CV studies demonstrated that PAH_{n+1}/PAA_n/POM Au electrodes have high stability, fast response and good electrocatalytic activity for the reduction of nitrite, chlorate and peroxodisulfate; making these electrodes potential candidates for durable electrochemical sensors for the detection of these molecules.

Acknowledgements

E.V. thanks CONICET and Tenaris for a joint scholarship. E.J.C. and F.J.W are CONICET Fellows. Financial support from CONICET, ANPCyT-Max Planck Gesselschaft Collaboration (Grant PICT-2006 No. 1146) and Universidad de Buenos Aires is gratefully acknowledged.

References

[1] R.W. Murray, Acc. Chem. Res. 13 (1980) 135.
[2] M.T. Pope, A. Müller, Angew. Chem. Int. Ed. Engl. 30 (1991) 34.
[3] M. Sadakane, E. Steckhan, Chem. Rev. 98 (1998) 219.
[4] G. Paliwoda-Porebska, M. Stratmann, M. Rohwerder, K. Potje-Kamloth, Y. Lu, A.Z. Pich, H.J. Adler, Corros. Sci. 47 (2005) 3216.
[5] S. Dong, Z. Jin, J. Chem. Soc., Chem. Commun. (1987) 1871.
[6] B. Wang, S. Dong, J. Electroanal. Chem. 328 (1992) 245.
[7] A. Kuhn, F.C. Anson, Langmuir 12 (1996) 5481.
[8] B. Keita, L. Nadjo, J. Electroanal. Chem. 191 (1985) 441.
[9] B. Keita, L. Nadjo, G. Krier, J.F. Muller, J. Electroanal. Chem. 223 (1987) 287.
[10] S. Dong, L. Cheng, X. Zhang, Electrochim. Acta 43 (1997) 563.
[11] B. Keita, K. Essaadi, L. Nadjo, J. Electroanal. Chem. 259 (1989) 127.
[12] M.-C. Pham, S. Bouallala, L.A. Lé, V.M. Dang, P.-C. Lacaze, Electrochim. Acta 42 (1997) 439.
[13] B. Keita, A. Belhouari, L. Nadjo, J. Electroanal. Chem. 355 (1993) 235.
[14] A. Papadakis, A. Souliotis, E. Papaconstantinou, J. Electroanal. Chem. 435 (1997) 17.
[15] P. Wang, X. Wang, G. Zhu, Electrochim. Acta 46 (2000) 637.
[16] M. Zhou, L.-P. Guo, F.-Y. Lin, H.-X. Liu, Analytica Chim. Acta 587 (2007) 124.
[17] W. Guo, L. Xu, B. Xu, Y. Yang, Z. Sun, S. Liu, J. Appl. Electrochem. 39 (2009) 647.
[18] B. Keita, A. Belhouari, L. Nadjo, R. Contant, J. Electroanal. Chem. 381 (1995) 243.
[19] P. Wang, Y. Li, J. Electroanal. Chem. 408 (1996) 77.
[20] L. Wang, D. Xiao, E. Wang, L. Xu, J. Coll. Int. Sci. 285 (2005) 435.
[21] C. Rong, F.C. Anson, Inorg. Chim. Acta 242 (1996) 11.
[22] G. Decher, Science 277 (1997) 1232.
[23] G. Decher, J.D. Hong, J. Schmitt, Thin Solid Films 210–211 (1992) 831.
[24] M. Ferreira, J.H. Cheung, M.F. Rubner, Thin Solid Films 244 (1994) 806.
[25] D. Laurent, J.B. Schlenoff, Langmuir 13 (1997) 1552.
[26] M. Tagliazucchi, E.J. Calvo, in: R.C. Alkire, D.M. Kolb, J. Lipkowski, P.N. Ross (Eds.), Chemically Modified Electrodes, Wiley-VCH Verlag GmbH & Co., Weinheim, 2009.
[27] J. Hodak, R. Etchenique, E.J. Calvo, K. Singhal, P.N. Bartlett, Langmuir 13 (1997) 2708.
[28] T.R. Farhat, J.B. Schlenoff, Langmuir 17 (2001) 1184.
[29] S. Han, B. Lindholm-Sethson, Electrochim. Acta 45 (1999) 845.
[30] C. Sun, J. Zhao, H. Xu, Y. Sun, X. Zhang, J. Shen, J. Electroanal. Chem. 435 (1997).
[31] L. Cheng, L. Niu, J. Gong, S. Dong, Chem. Mater. 11 (1999) 1465.
[32] D.M. Fernandes, H.M. Carapuça, C.M.A. Brett, A.M.V. Cavaleiro, Thin Solid Films 518 (2010) 5881.
[33] T.C. Wang, M.F. Rubner, R.E. Cohen, Langmuir 18 (2002) 3370.
[34] M. Vago, M. Tagliazucchi, F.J. Williams, E.J. Calvo, Chem. Commun. (2008) 5746.
[35] M. Tagliazucchi, F.J. Williams, E.J. Calvo, J. Phys. Chem. B 111 (2007) 8105.
[36] R.M.A. Azzam, N.M. Bashara, Ellipsometry and Polarized Light, North Holland Publishing Company, Amsterdam, 1977.
[37] J.H. Scofield, J. Electron Spectrosc, Relat. Phenom. 8 (1976) 129.
[38] E.J. Calvo, C. Danilowicz, R. Etchenique, J. Chem. Soc., Faraday Trans. 91 (1995) 4083.
[39] G.Z. Sauerbrey, Z. Phys. 155 (1959) 206.
[40] H.O. Finklea, D.A. Snider, J. Fedyk, Langmuir 6 (1990) 371.
[41] S.S. Shiratori, M.F. Rubner, Macromolecules 33 (2000) 4123.
[42] I.V. Kozhevnikov, Catalysis by Polyoxometalates, John Wiley & Sons, Ltd., Sussex, 2002.
[43] M. Fournier, C. Rocchiccioli-Deltcheff, L.P. Kazansky, Chem. Phys. Lett. 223 (1994) 297.
[44] H. Ratajczak, A.J. Barnes, A. Bielanski, H.D. Lutz, A. Müller, M.T. Pope, in: M.T. Pope, A. Müller (Eds.), Polyoxometalate Chemistry, Kluwer Academic Publishers, 2001.
[45] G.P. Girina, E.V. Ovsyannikova, N.M. Alpatova, Russ. J. Electrochem. 43 (2007) 1026.
[46] J. Wang, Analytical Electrochemistry, Wiley-VCH, New Jersey, 2006.
[47] A.J. Bard, L.R. Faulkner, Electrochemical methods, Fundamentals and Applications, John Wiley & Sons, New Jersey, 2001.